

# Effect of Thermal Ageing Characteristics of Al-Si-Fe/SiC Particulate Composite Synthesized by Double Stir Casting

V.S. Aigbodion\* and S.B. Hassan

\* Department of Metallurgical and Materials Engineering, Ahmadu Bello University, Samaru, Zaria, Nigeria

Received 3 June 2009; accepted 6 September 2009

تأثير خواص التقادم الحراري لتكوين جزيئات Al-Si-Fe/SiC المصنعة بواسطة الصب المضاعف

فا . س . أيجبوديون ، س . ب . حسان

**الغلامه:** تأثير التقادم الحراري على الانشاءات الميكروية و مواصفات 10wt% and 20wt%SiC جزيئات مسلحه Al-Si-Fe مصفوفة مركبه ، منتج ، بواسطة طريقة الصب الثنائي قد تمت دراسته. النماذج المركبة قد عوملت بالخليط المعامل حراريا على درجة 500 مئوية لمدة ثلاث ساعات وتم تقادمه على 300، 200، 100 درجة مئوية مع تقادم الوقت لمدته 60 الى 660 دقيقة. خواص التقادم لهذه المركبات قد تم تقييمها بواسطة قيم الصلادة، طاقة الاصطدام، خواص الشد، وكذلك التركيب المايكروي. قيم قوة الشد تحصل على صلادة تزداد بزيادة نسبة اكارييد السلكون في السبيكة بزيادة طاقة الاصطدام في كل من الصب و تصلب النماذج المتقادمة حراريا. إن زيادة قيم الصلادة و القوة لأثناء التقادم الحراري تعزى الى تكوين ترسبات منتظمة و متصلة في شبكة المعدن. تم اكتشاف ان كل من المركبات المصنفة قد بينت تعجيل في التقادم الحراري مقارنة بالسبيكات المنتجة. ومع ذلك فإن 20wt% SiC المسلح المركب يبين تعجيل أكثر بالمقارنة الى: 10wt% SiC المسلح المركب.

**المفردات المفتاحية:** Al-Si-Fe/SiC ، تقادم حراري ، مركب ، خواص ميكانيكية ، تركيب ما يكرين ترسيب .

**Abstract:** The effect of thermal ageing on the microstructure and properties of 10wt% and 20wt%SiC particulate reinforced Al-Si-Fe matrix composite, produced by double stir casting route, have been studied. The composite samples were solution heat-treated at 500°C for 3 hrs and aged at 100, 200, and 300°C with ageing time between 60 and 660 minutes. The ageing characteristics of these grades of composite were evaluated using hardness values, impact energy, tensile properties and microstructure. The tensile strength, yield strength, hardness values increased as the percentage of silicon carbide increased in the alloy with decreased impact energy in both the as-cast and thermally age-hardened samples. The increases in hardness values and strength during thermal ageing are attributed to the formation of coherent and uniform precipitation in the metal lattice. It was found that both grades of composites showed acceleration in thermal ageing compared to the monolithic alloy. However, the 20wt%SiC reinforced composite showed more acceleration compared to 10wt%SiC reinforced composite.

**Keywords:** Al-Si-Fe/SiC, Thermal ageing, Composite, Mechanical properties, Microstructure and precipitation

## 1. Introduction

In recent years, the development of metal matrix composites (MMCs) has been receiving worldwide attention on account of their superior strength and stiffness in addition to high wear resistance and creep resistance compared to their corresponding wrought alloys. The ductile matrix permits the blunting of cracks and stress concentrations by plastic deformation and provides a material with improved fracture toughness (Aigbodion. V.S, 2007).

The present trend, therefore, seems to be towards the development of discontinuously reinforced metal matrix composites which are gaining widespread acceptance primarily because they have recently become available at a

relatively low cost compared to uni-and multi-directional continuous-fiber reinforced MMCs and the availability of standard or near-standard metal working methods which can be utilized to form these MMCs (Aigbodion, V.S, 2007, and Clyne, T. W, 2000).

Nowadays, research all over the globe is focusing mainly on Aluminium (Aigbodion, V.S., 2007, and Yaro, S.A., et al. 2006) because of its unique combination of good corrosion resistance, low density and excellent mechanical properties. The unique thermal properties of Aluminium composites such as metallic conductivity with a coefficient of expansion that can be tailored down to zero, add to their prospects in aerospace and avionics (Sagail, A. and Leisk, G, 1992).

\*Corresponding author's e-mail: aigbodionv@yahoo.com

The age-hardening characteristics of an alloy are generally modified by the introduction of reinforcement. These modifications are due to the manufacturing process, the reactivity between the reinforcement and the matrix, the size, the morphology and volume fraction of the reinforcement (Sagail, A., Leisk, G., 1992; Rajan, T.V. and Sharma, C.P, 1988).

In contrast to this extensive data available on the heat treatment of Al-Si-Fe alloys with convectional alloying elements (Yaro, S.A., *et al.* 2006). Relatively little is demanded for their ageing hardening characteristics particularly in Silicon carbide reinforcement (Aigbodion, V.S., 2007). Hence, there is need for research to be carried out in this very important area. The aims of the present research are to determine the microstructure and thermal ageing characteristics of Al-Si-Fe/SiC particulate composites with a view to obtaining the optimum thermal age hardening procedure that would enable the achievement of the desired mechanical properties.

## **2. Experimental Procedure**

### **2.1 Materials**

The experimental materials used in this study included: silicon carbide with an average particle size of 10 $\mu$ m, ferrosilicon, high purity aluminium electrical wire obtained from Northern Cable Company NOCACO (Kaduna), moulding boxes, silica sand, and bentonite obtained from National Metallurgical Development Centre, Jos, Nigeria.

### **2.2 Equipment**

The equipment used in this study included: pyrometer, mechanical stirrer, a crucible, an electrical resistance furnace, a Rockwell hardness tester, a Charpy impact machine, a Tinus Olsen tensile machine and a Metallurgical microscope with a built-in camera.

## **3. Methods of Sample Production**

The synthesis of the metal matrix composite that was used in this research was achieved using a double stir-casting method at the Foundry Shop of the National Metallurgical Development Center, Jos, Nigeria. The samples were produced by keeping the percentage of iron and silicon constant, reinforced with Silicon carbide particles of 10wt% and 20wt%. High-purity aluminium electrical wires was charged in a graphite crucible kept in an electric resistance furnace and 0.01%NaCl-KCl powder were used as a cover for melting the alloy in order to minimize oxidation of aluminium by excluding oxygen and creating a protective atmosphere inside the furnace. After the melting of the pure aluminium, the temperature of the furnace was raised to 720°C for the purpose of superheating the aluminium melt. The required quantity of 2.8% silicon and 0.8%iron was added to the melt using ferrosilicon, and the melt was thoroughly stirred (Aigbodion, V.S., 2007; Aigbodion,V.S. and Hassan, S.B., 2007).

With progressive melting, the furnace temperature was raised to 780°C and the melt was held at this temperature for 10 minutes. The melt was then skimmed to remove the oxides and impurities. The molten metal was continuously stirred in order to ensure a near-uniform distribution of alloying elements and prevent the elements from settling at the bottom due to their higher density. For each melting, 200g of charge materials was used to produce the alloy. The Silicon carbide particles were preheated to 1000°C, to make their surface oxidized (Aigbodion, V.S. and Hassan, S.B., 2007).

The alloy was then cooled down to a temperature just below the liquidus point (580°C) to keep the slurry in a semi-solid state. At this stage the preheated SiC particles were added and mixed manually. Manual mixing was used because it was very difficult to mix using automatic device when the alloy was in a semi-solid state. After manual mixing was done, the composite slurry was reheated to a temperature of 720°C and then automatic mechanical mixing was carried out for about 20 minutes at an average stirring speed of 150 rpm. In the final mixing processes, the furnace temperature was controlled between 730 and 740°C and the pouring temperature was controlled to about 720°C (Aigbodion, V.S., 2007; Aigbodio, V.S and Hassan, S.B., 2007). A preheated sand mould with diameter 18 mm and 300mm length was used to produce cast bars. After casting, the samples were machined into tensile, impact and hardness test specimens for the purpose of determining the mechanical properties.

## **4. Heat Treatment of the Samples**

The test samples were solution heat-treated at temperature of 500°C in an electrically heated furnace, soaked for 3 hours at this temperature and then rapidly quenched in warm water at 65°C. Thermal ageing of the test samples was carried out at temperatures of 100, 200 and 300°C, for various ageing times of 60 to 660 minutes, and then cooled in air. The thermal ageing characteristic of these grades of composites was evaluated using hardness values obtained from solution heat-treated samples of the investigated composites subjected to the aforementioned temperature conditions. The tensile and impact tests were conducted at the peak ageing time of the various ageing temperatures (Aigbodion, V.S., 2007; Rajan, T.V. and Sharma , C.P., 1988).

## **5. Determination of Hardness Values**

The hardness values of the samples were determined according to the provisions in ASTM E18-79 using the Rockwell hardness tester on "B" scale (Frank Well test Rockwell Hardness Tester, model 38506) with a 1.56 mm steel ball indenter, minor load of 10kg, major load of 100kg and hardness value of 101.2 HRB as the standard block. Before the test, the mating surfaces of the indenter, plunger rod and test samples were thoroughly cleaned by removing dirt, scratches and oil and the testing machine

**Table 1. Hardness (HRB) values for as-cast and thermal age-hardened with 10wt% and 20wt% of silicon carbide**

wt% SiC	As-cast	Peak aged at 100°C	Peak aged at 200°C	Peak aged at 300°C
0	31.1	60.1	61.5	62.0
10	57.2	75.0	74.5	84.0
20	67.0	86.0	87.0	89.0

**Table 2. Yield strength of Al-Si/SiC composites with 10wt% and 20wt% of silicon carbide**

Wt% SiC	As-cast (N/mm <sup>2</sup> )	Peak aged at 100°C (N/mm <sup>2</sup> )	Peak aged at 200°C (N/mm <sup>2</sup> )	Peak aged at 300°C (N/mm <sup>2</sup> )
0	45.60	59.90	56.40	52.40
10	68.46	73.35	75.00	73.00
20	79.98	80.75	82.50	80.34

**Table 3. Tensile strength of Al-Si-Fe/SiC composites with 10wt% and 20wt% of silicon carbide**

Wt % SiC	As-cast (N/mm <sup>2</sup> )	Peak aged at 100°C (N/mm <sup>2</sup> )	Peak aged at 200°C (N/mm <sup>2</sup> )	Peak aged at 300°C (N/mm <sup>2</sup> )
0	58.69	62.50	67.18	64.20
10	96.06	98.50	98.50	100.20
20	106.12	120.43	125.00	121.85

was calibrated using the standard block. The samples were placed on anvils, which acted as support for the test samples. A minor load of 10kg was applied to the sample in a controlled manner without inducing impact or vibration and the zero datum position was established. The major load of 100 kg was then applied, and the reading was taken when the large pointer came to rest or had slowed appreciably and dwelled for up to 2 seconds. The load was then removed by returning the crank handle to the latched position and the hardness value read directly from the semi automatic digital scale. Three indentations were taken and the average represents the hardness values (Aigbodion, V.S., 2007 and Metal handbook., 1985).

## 6. Determination of the Tensile Properties

The tensile properties of the as-cast and peaking thermal ageing samples were conducted on Tinus-Olsen tensile testing machine with a strain rate of .002S<sup>-1</sup>. The test pieces were machined to the standard shape and dimensions as specified by the American Society for Testing and Materials (Annual Books of ASTM Standards, 1990). The sample was locked securely in the grips of the upper and lower crossbeams of the testing machine. A small load was initially applied to seat the sample in the grips and then the load was increased until failure occurred.

## 7. Impact Strength Determination

The impact test of the as-cast and peaking thermal ageing samples was conducted using a fully instrumented Avery Denison test machine. The mass of the hammer was 22.7 kg and the striking velocity was 3.5 m/sec. Charpy impact tests were conducted on notched samples. Standard square impact test sample measuring 75 x 10 x

10 mm with notch depth of 2 mm and a notch tip radius of 0.02 mm at an angle of 45° was used (Annual Books of ASTM Standards, 1990).

Before the test sample was mounted on the machine, the pendulum was released to calibrate the machine. The test samples were then gripped horizontally in a vice and the force required to break the bar was released from the freely swinging pendulum. The value of the angle through which the pendulum had swung before the test sample was broken corresponded with the value of the energy absorbed in breaking the sample and this was read from the calibrated scale on the machine (Annual Books of ASTM Standards, 1990).

## 8. Microstructural Examination

Metallographic samples were cut from the produced samples. The cut samples were then mounted in Bakelite, and mechanically ground progressively on grades of SiC-impregnated emery paper (80-600 grits) sizes using water as the coolant. The ground samples were then polished using one-micron size alumina polishing powder suspended in distilled water. Final polishing was done using 0.5 micron alumina polishing powder suspended in distilled water. Following the polishing operation, etching of the polished specimen was done using Keller's reagent. The structure obtained was photographically recorded using an optical microscope with built-in camera (Aigbodion, V.S., 2007; Aigbodion, V.S. and Hassan. S.B., 2007).

## 9. Results and Discussion

### 9.1 Results

The various microstructures developed for the two grades of composites in the as-cast and thermally age-

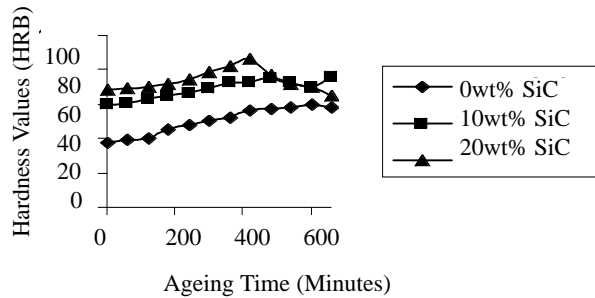


**Figure 1. Variation of hardness values with ageing time at ageing temperature of 100°C**

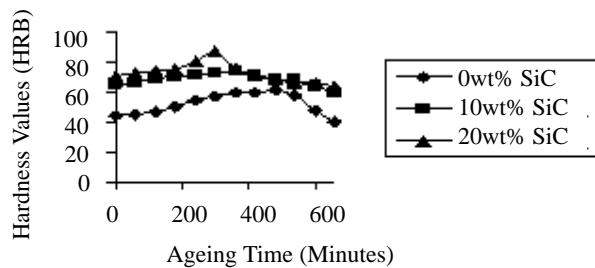


**Figure 2. Variation of hardness values with ageing time at ageing temperature of 200°C**

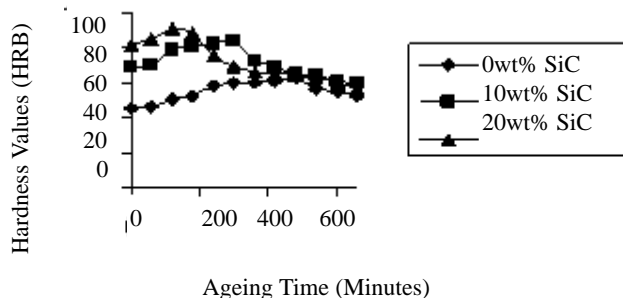


**Figure 3. Variation of hardness values with ageing time at ageing temperature of 300°C**

hardened condition are shown in Micrographs 1-12. The thermal ageing response measured by the variation of hardness with time for two grades of composites is shown in Figs. 1-3. Table 1 shows the hardness values of both the thermally as-cast and age-hardened Al-Si-Fe/SiC composites. The results of yield strength and ultimate tensile strength with weight fraction of Silicon carbide at various ageing temperatures are shown in Tables 2-3. The results of impact energy with weight fraction of Silicon carbide (SiC) at various ageing temperatures are shown in Table 4.

## 10. Discussions

### 10.1 Thermal Ageing Characteristics of Al-Si-Fe/SiC Composites

From Figs. 1-3, it can be seen that there is a steep rise in the hardness values of each grade of the composite at

initial stages for all ageing temperatures and then a fall after reaching the various peak ageing times are reached, corresponding to over-ageing. However, at higher ageing temperature the materials developed peak hardness at shorter ageing time, because the rate of precipitation of the second phase materials is faster and hence increases in hardness values. The time to obtain peak hardness is shorter according to the sequence: 100°C > 200°C > 300°C (See Figs. 1-3).

The thermal age-hardening behavior of the Al-Si-Fe/SiC particulate composites are similar to Al-Si-Mg/SiC particulates as reported by Cottu *et al.* (1992) *ie.* hardness continuously increases to a maximum during thermal ageing and then decreases later due to over ageing. It is interesting to note that in the reinforced aluminium alloy metal-matrix, as the volume fraction of SiC increase to 20wt% in the aluminium alloy there is a monotonic reduction in the time required to reach peak hardness (See Fig. 3).

The 20wt%SiC addition, yielded the highest hardness value. As far as hardening behavior of the composites is concerned, particle addition in the matrix alloy increases the strain energy in the periphery of the particles in the matrix and these tendencies may be due to the formation of the dislocation at the boundary of the ceramic particles by the difference in the thermo-expansion coefficient between the matrix and ceramic particles during solution treatment and quenching since a lot of dislocations generate in the main matrix/particle interface (Bedir, F., 2006). Thus, dislocations cause the hardness increase in composite as well as residual stress increase because it acts as non-uniform nucleation sites in the interface following the age treatment. It is thought that the higher the amount of the ceramic particles in the matrix, the higher the density of the dislocation, and as a result, the higher the hardness of the composite.

### 10.2 Microstructural Analysis

Microstructures of the as-cast and heat-treated composites at various ageing temperatures and peaking ageing time were examined by the use of a metallurgical microscope. They were observed to contain primarily  $\alpha$ -Al, silicon eutectic and SiC particle as shown in Micrographs 1-12. In the microstructure of the composites Si phase was seen apparently in the eutectic regions, and intermetallic compounds such as FeSiAl<sub>3</sub>, iron-containing phases due to the secondary alloying elements (Aigbodion, V.S., 2007; Rajan, T.V. and Sharma, C.P, 1988).

The microstructure of the as-cast unreinforced Al-Si-Fe alloy is shown in Micrograph 1, while Micrographs 2-3 show the microstructure of the as-cast reinforced alloys with SiC particles.

The microstructure reveals that there are small discontinuities and a reasonably uniform distribution of SiC particles. The ceramic phase is shown as dark phase, while the metal phase is white. These structures are in agreement with the co-continuous interlaced phases studied by other researchers (Rohatgi, P.K., *et al.* 1988 and Whitehouse, A.F., 1990). Micrographs 4-12, show the

**Table 4. Impact energy for as-cast and age-hardened with 10wt# and 20wt# of silicon carbide**

Wt% SiC	As-cast	Peak aged at 100°C	Peak aged at 200°C	Peak aged at 300°C
0	17.0J	28.0J	24.0J	22.0J
10	14.5J	20.0J	19.0J	19.0J
20	12.0J	17.0J	15.5J	16.0J

microstructure of the thermally age-hardened Al-Si-Fe/SiC composites. The microstructure reveals the dissolution and distribution of the SiC particles in the metal matrix and the presence of precipitates at the particles matrix interfaces with precipitation and dissolution of the SiC particles and silicon eutectic phase (Aigbodio, V.S., 2007; Aigbodio, V.S. and Hassan, S.B., 2007).

The formation and presence of precipitates at the particles- matrix interfaces may be appreciated by comparing micrographs of the composite in the as-cast state micrographs 1-3 and in the peak age-hardened state micrographs 4-12. The micrographs in the peak age-hardened state reveal precipitates covering the surface at the particles-matrix interfaces. Cottu *et al.* (1992) reported a similar behavior of increased precipitation at interfaces for aluminum alloy 6061 reinforced with whiskers of silicon carbide.

### 10.3 Hardness Value

From Table 1, the hardness values for thermally as-cast and age-hardened composite increases as the percentage of Silicon carbide increases from 10wt% to 20wt% in the alloy. This is due to an increase in the percentage of the hard and brittle phase of the ceramics body in the alloy.

The hardness values of the thermally age-hardened alloy are almost equal at various ageing temperatures with percentage SiC additions (See Table 1), in line with the earlier observation of (Cottu *et al.* 1992 and Ikechukwuka 1997).

### 10.4 Yield and Tensile Strength

From Tables 2-3, the yield strength and ultimate tensile strength of both the as-cast and age-hardened composites increased with the increased percentage silicon carbide to 20 wt% SiC. The as-cast samples have a value of 79.98 and 106.12N/mm<sup>2</sup> for yield and tensile strength at 20% SiC addition.

For the thermally age-hardened samples, similar trends were also observed as for the case of the as-cast samples, in that the yield strength and ultimate tensile strength increased to 20% wt of SiC. The ultimate tensile strengths of the thermally age-hardened samples at 20 wt% SiC are 120.43, 125.00 and 121.85N/mm<sup>2</sup> at peak ageing of 100, 200 and 300°C respectively. (See Table 3). Also the yield strengths of age-hardened samples at 20 wt% SiC addition are 80.75, 82.50 and 80.34N/mm<sup>2</sup> at peak ageing of 100, 200 and 300°C respectively (See Table 2).

The higher values of both ultimate tensile strength and yield strength obtained at 20 wt% SiC are attributed to the uniform distribution of the SiC particles in the microstructure of the 20 wt% SiC (See Micrographs 3, 10-12). It can

be seen that the inter-particle distance is smaller. The contribution of inter-particle distance to strain hardening arises from the fact that the space permitted a dislocation to maneuver round obstacles limits the yield stress given by the formula (Dieter, G.E., 1988):

$$\delta = \frac{Gb}{\lambda} \cdot \delta = \text{Yield stress, } \delta = \text{Inter-particle distance,}$$

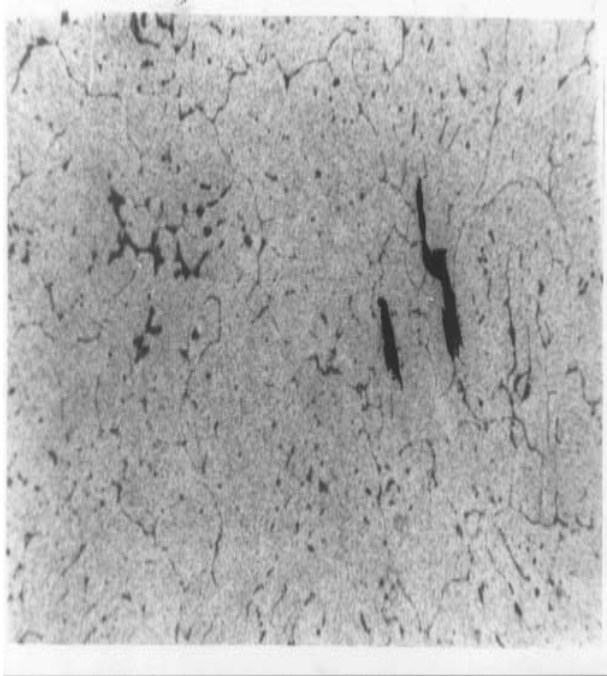
G = Shear energy of dislocation and b = Burger vector.

The smaller the values of  $\lambda$  the greater the yield stress as a result of strain hardening. It therefore supports the fact that (Micrographs 3,10-12) with smaller  $\lambda$ .

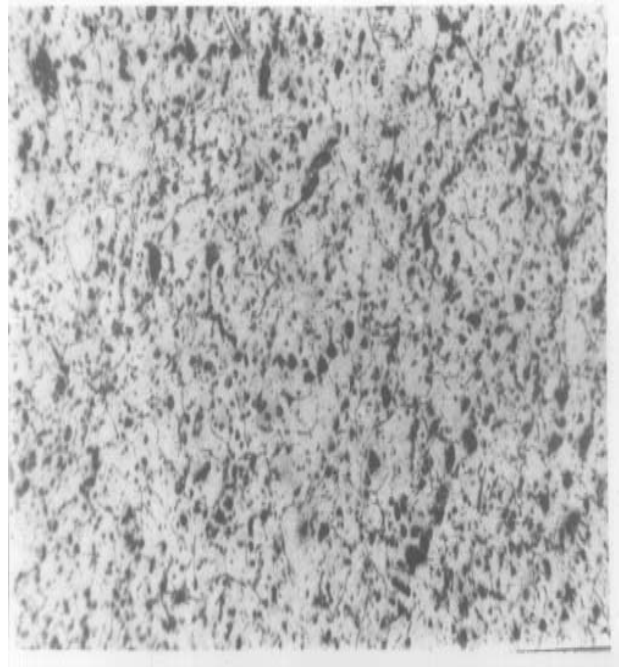
A substantial increase in both the yield strength and ultimate tensile strength was obtained when compared with the results of as-cast samples. For example the yield strength of Al-Si-Fe/10SiC particles increased from 68.46 to 75.00N/mm<sup>2</sup>, while the ultimate tensile strength increased from 96.06 to 98.50N/mm<sup>2</sup> in the as-cast and peak age-hardened at 200°C respectively. The yield and tensile strength of Al-Si-Fe/20SiC particles also increased from 79.98 to 82.50 N/mm<sup>2</sup> and 106.12 to 125.00 N/mm<sup>2</sup> in the as-cast and thermally age-hardened at 200°C temperature (See Tables 2-3).

These results show that the Al-Si-Fe/10SiC particles samples has 9.55% and 2.54% increases in yield strength and ultimate tensile strength respectively over those of the as-cast samples at peak ageing at 200°C, while for the Al-Si-Fe/20SiC particles the respective increments were 3.15% and 17.79% for yield strength and ultimate tensile strength. The increase in strength of the thermally age-hardened samples over those of the as-cast are attributed to the uniform distribution of SiC in the aged samples than the as-cast samples respectively (See Micrographs 1 and 3 and Micrographs 4-12).

Sagail and Leisk (1992) and Whitehouse *et al.* (1991) attributed this to an increase in dislocation density at the interfaces. An increase in dislocation density strain hardens the metal-matrix locally and provides heterogeneous nucleation sites for precipitation, thereby accelerating the ageing response. The modulated structures formed during ageing in these grades of composites enhanced these properties and this is in agreement with the earlier works on Al-Si-Mg/SiC (Cottu, J.P. *et al.* 1992 and Ikechukwuka. N.A, 1997). The addition of SiC particles affects not only the precipitation kinetics but also the relative amounts of the various phases present in the microstructure. Besides during quenching from the solution heat treatment temperature, the SiC particles cool more slowly than the matrix (since the particles have a lower thermal conductivity). This causes the matrix around the particles to be



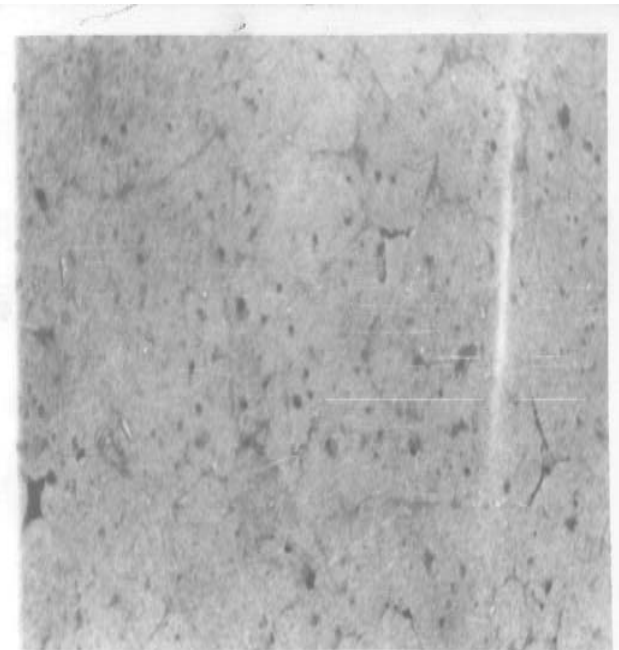
**Micrograph 1.** Microstructure of the Al-Si-Fe alloy, showing silicon eutectic (black) containing  $\text{FeAl}_3\text{Si}$  phases and  $\alpha\text{-Al}$  (white) (x200). The structure reveals the eutectic silicon containing  $\text{FeSiAl}_3$  phase in aluminium matrix.



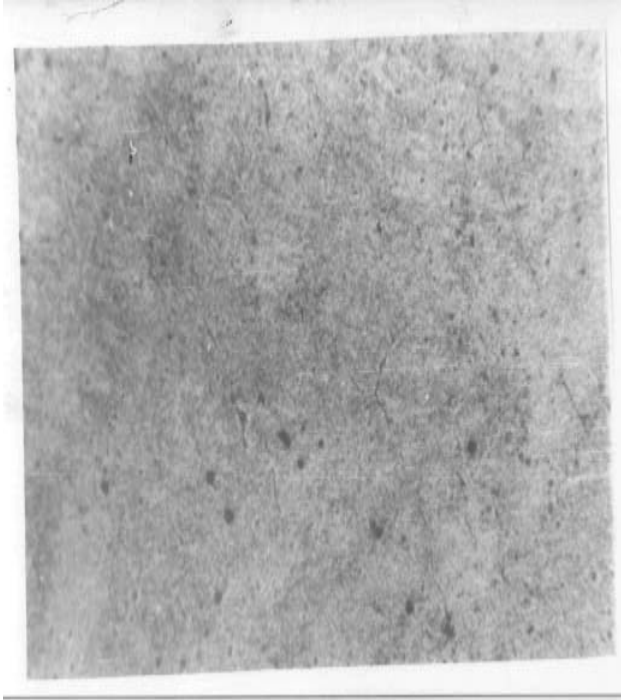
**Micrograph 3.** Microstructure of Al-Si alloy reinforced with 20 wt% of SiC. The structure reveals dissolution of the eutectic silicon phase and uniform distribution of SiC (black) in  $\alpha\text{-Al}$  matrix (white) (x200).



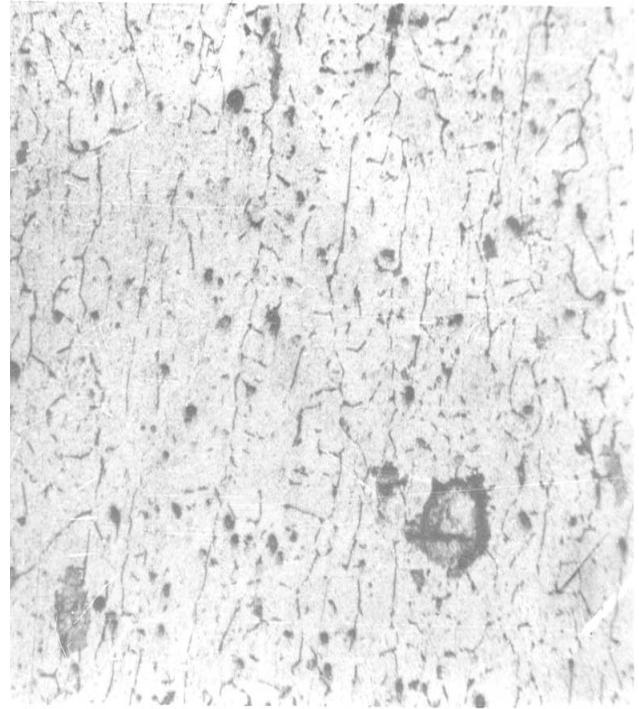
**Micrograph 2.** Microstructure of the Al-Si-Fe alloy with 10 wt% of SiC the the structure reveals the dissolution of the eutectic silicon phase and uniform distribution of SiC (black) in  $\alpha\text{-Al}$  matrix (white) (x200).



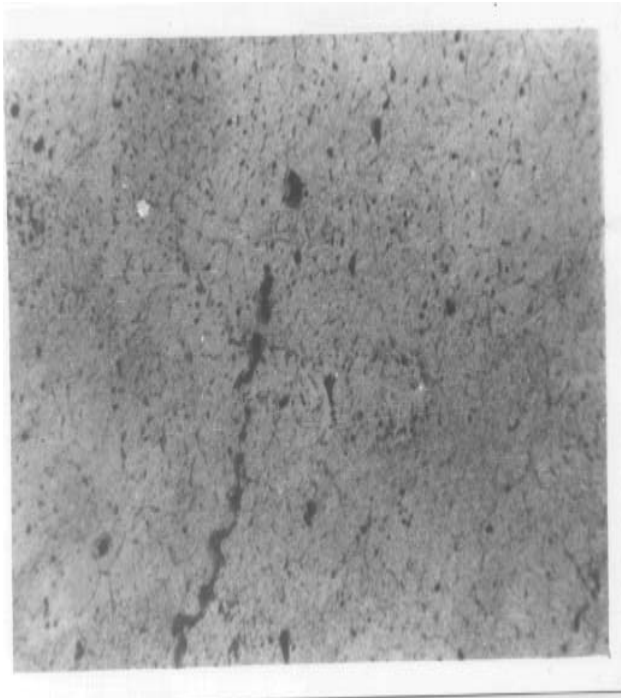
**Micrograph 4.** Microstructure of the Al-Si-Fe alloy after peak aged at  $100^\circ\text{C}$  (x200). The structure reveals dissolution and precipitation of the silicon eutectic (black) and the  $\text{FeAl}_3\text{Si}$  phases in  $\alpha\text{-Al}$  matrix (white).



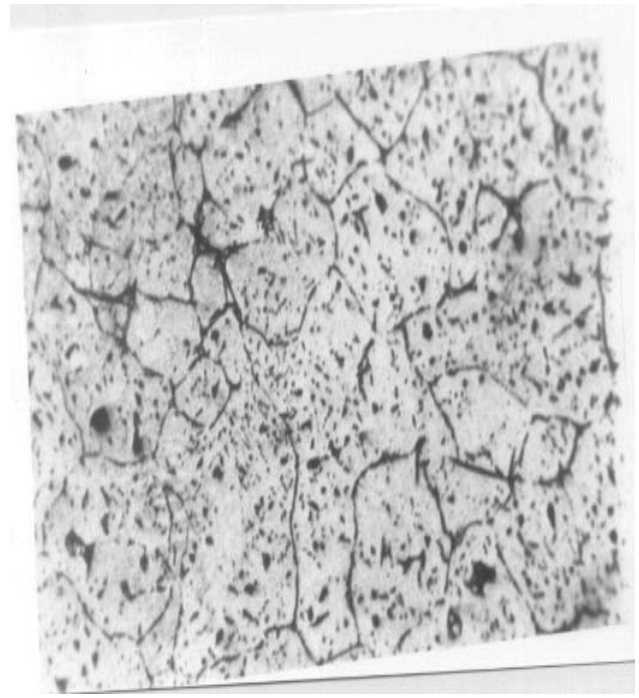
**Micrograph 5.** Microstructure of the Al-Si-Fe alloy after peak aged at 200°C (x200). The structure reveals uniform dissolution and precipitation of the silicon eutectic (black) and the FeAl<sub>3</sub>Si phases in α-Al matrix (white).



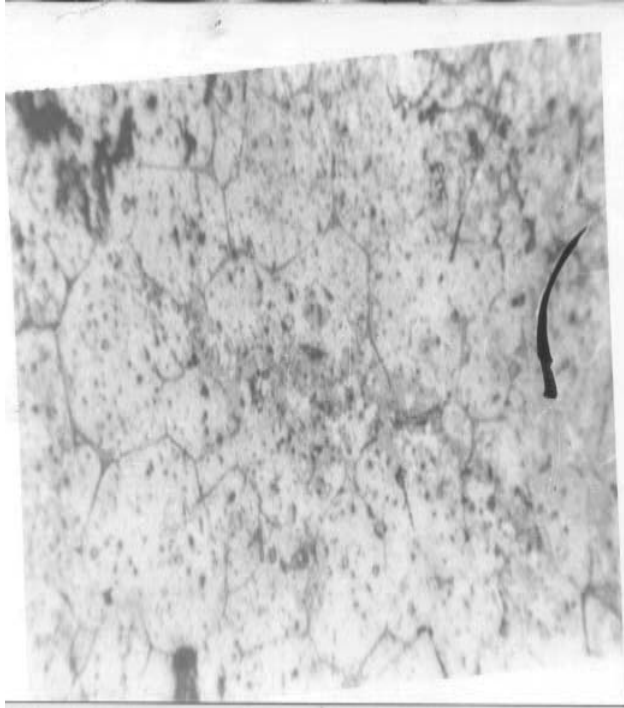
**Micrograph 7.** Microstructure of the reinforced alloy (10 wt% of SiC) after peak aged at 100°C (x200). The structure reveals the dissolution of the eutectic silicon phase and uniform distribution of SiC (black) in α-Al matrix (white).



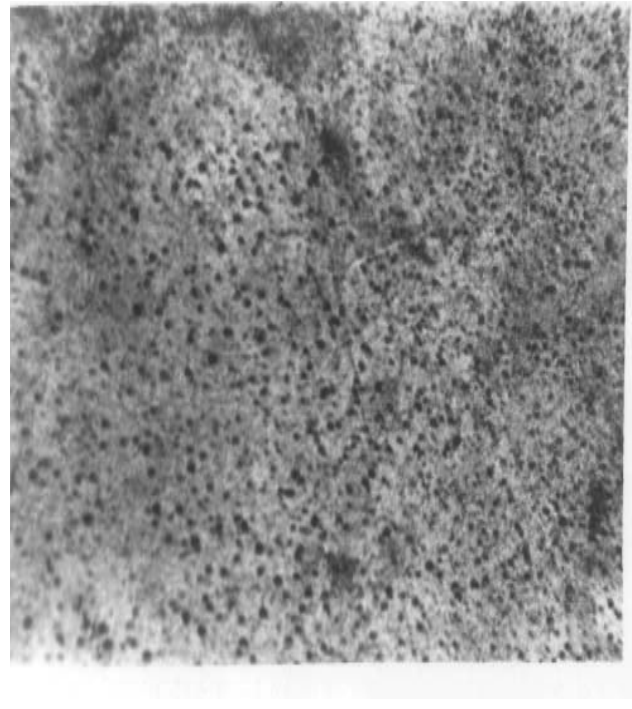
**Micrograph 6.** Microstructure of the unreinforced alloy after peak aged at 300°C (x200). The structure reveals dissolution and precipitation of the silicon eutectic (black) and the FeAl<sub>3</sub>Si phases with some segregation of silicon eutectic phases in α-Al matrix (white).



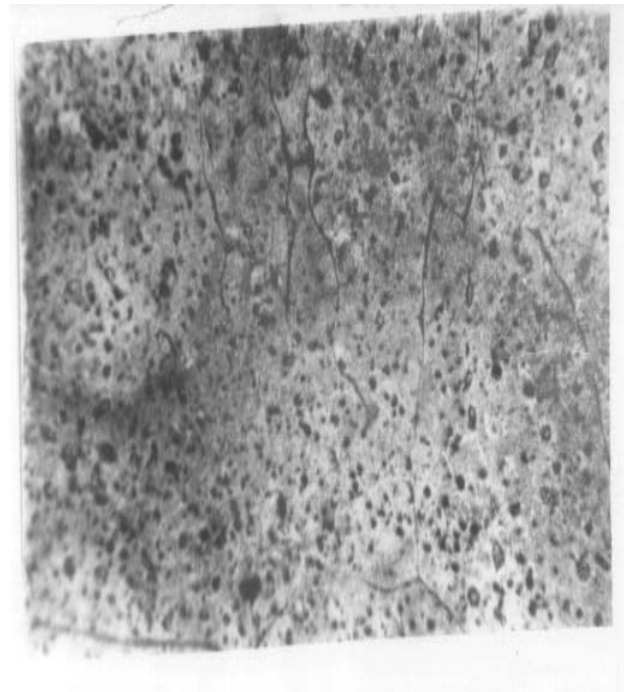
**Micrograph 8.** Microstructure of the reinforced alloy (10 wt% after peak aged at 200°C (x200). The structure reveals the dissolution of the eutectic silicon phase and distribution of SiC (black) in α-Al matrix (white).



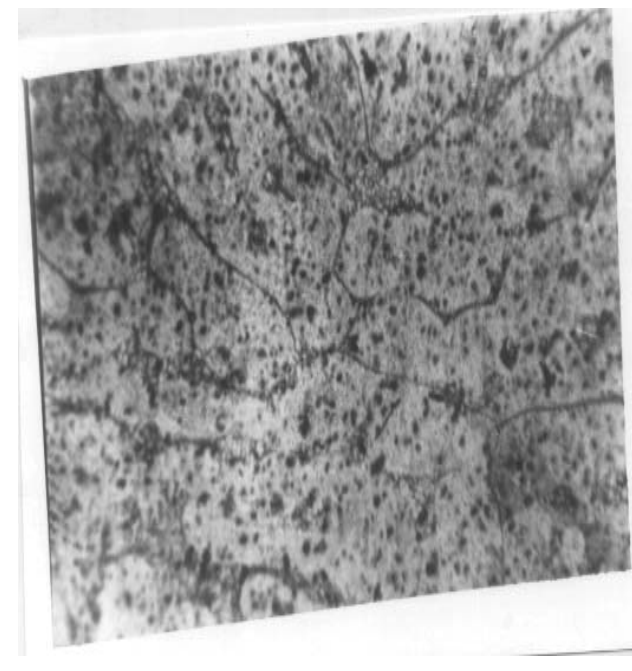
**Micrograph 9.** Microstructure of the reinforced alloy (10 wt% of SiC after peak aged at 300°C (x200). The structure reveals the dissolution of the eutectic silicon phase and uniform distribution of SiC (black) with precipitation of the SiC particles.



**Micrograph 11.** Microstructure of the reinforced alloy (20 wt% of SiC) after peak aged at 200°C (x200). The structure reveals the dissolution of the eutectic silicon phase and well uniformly distribution of SiC (black) with precipitation covering the aluminium phase (white).



**Micrograph 10.** Microstructure of the reinforced alloy (20 wt% of SiC) after peak aged at 100°C (x200). The structure reveals the dissolution of the eutectic silicon phase and uniform distribution of SiC (black) with precipitation covering.



**Micrograph 12.** Microstructure of the reinforced alloy (20 wt% of SiC) after peak aged at 300°C (x200). The structure reveals the dissolution of the eutectic silicon phase and uniform distribution of SiC (black) with precipitation covering.

warmer than the bulk matrix. The high dislocation density and the high solubility centers (the warm particles-matrix interfaces) in the composite are favorable conditions for precipitation formation. This mechanism is a possible explanation for the higher volume fraction of precipitates obtained in the composite of the age hardening condition (Aigbodion, V.S., 2007; Aigbodion, V.S. and Hassan, S.B., 2007).

### 10.5 Impact Energy

From the Table 4, the impact energy of both the as-cast and age-hardened samples, decreased as the percent SiC addition increases in the alloy. The brittle nature of the reinforcing materials (SiC) plays a significant role in degrading the impact energy of the composite, since the unreinforced alloy and the alloy with 10wt% SiC particles have the highest impact energy, indicating that they are the toughest of them all (Aigbodion, V.S., 2007).

## 11. Conclusions

From the results of the investigations, the following conclusions have been made:

- 1) The uniform distribution of the SiC particles in the microstructure of both the as-cast and thermally age-hardened Al-Si-Fe/SiC composites is the major factor responsible for the improvement in the mechanical properties.
- 2) The addition of SiC particles affects not only the precipitation kinetics but also the relative amounts of the various phases present in the microstructure, and that during quenching from the solution heat treatment temperature, the SiC particles cool more slowly than the matrix (since the particles have a lower thermal conductivity). This causes the matrix around the particles to be warmer than the bulk matrix. The high dislocation density and the high solubility centers (the warm particles-matrix interfaces) in the composite are favorable conditions for precipitation formation. This mechanism is a possible explanation for the higher volume fraction of precipitates obtained in the composite of the age-hardening condition.
- 3) This research therefore, has established that these grade of composites respond to precipitation-hardening heat treatment.

## References

Aigbodion, V.S., 2007, "Development of Al-Si-Fe/SiC Particulate Composite as advanced Materials for

- Engineering Applications," M.Sc Thesis, Department of Metallurgical Engineering, Ahmadu Bello University, Zaria, Nigeria, pp. 45-50.
- Aigbodion, V.S. and Hassan, S.B., 2007, "Effect of Silicon Carbide Reinforcement on Microstructure and Properties of cast Al-Si-Fe/SiC Particulate Composites," *Materials Science and Engineering A*: 447, pp. 355-360.
- Annual Books of ASTM Standards, 1990, Section 1. Iron and Steel Products, Vol. 261 01.04, pp. 13-63.
- Bedir, F., 2006, "Fabrication of Two Layered Al-B4C Composites by Conventional Hot Pressing under Nitrogen Atmosphere and their Characterization," *J. of Mech.Sci. and Tech. KSME*, Vol. 20(7), pp. 1002-1011
- Clyne, T.W., (ed.), 2000, "Comprehensive Composite Materials," Vol. 3, Metal Matrix Composites (ser. eds), pp. 1-8.
- Cottu, J.P., Couderc, J.J., Viguier, B. and Bernard, L., 1992, "J. Mater Sci 27," pp. 3068-3074.
- Dieter, G.E., 1988, "Mechanical Metallurgy," McGraw-Hill Company, pp. 184-223.
- Fishman, S.G. and Dhingra, A.K., 1988, "Reinforced Metal Composites," *Materials Park, OH: ASM International Publication*, p. 249.
- Ikechukwuka, N.A., 1997, "Characterization of Aluminium Alloy 2618 and Its Composites Containing Alumina Particles," unpublished PhD thesis Department Mechanical Engineering, University of Saskatchewan, Saskatoon, pp. 87-200.
- Metals handbook, Mechanical testing, 1985, 9th edition, Vol. 8, American Society for Metals, the United States of America, pp. 250-257
- Rajan, T.V. and Sharma, C.P., 1988, "Heat Treatment Principles and Techniques," Published by Prentice-hall of India Private Limited, pp. 35-159.
- Rohatgi, P.K., Yarandi, F.M. and Liu, Y., Proc. of Inter. Symposium on Advances in Cast.
- Sagail, A., Leisk, G., 1992, "Heat Treatment Optimization of Alumina/Aluminium Metal Matrix Composites using the Taguchi Approach," *Scripta Metallurgica et Materials*, pp. 871-876.
- Yaro, S.A., Aigbodion, V.S. and Mohammed, O.Y., "Effects of Copper Addition on the Mechanical Properties of Al-Si-Fe Alloy," *International Research Journal in Engineering & Technology (IREJEST) FUTO*, Owerri, Nigeria, pp. 32-39.
- Whitehouse, A.F., Shahani, R. A. and Clyne, T.W., 1991, *Metal Matrix Composites: Processing, Microstructure and Properties*, 12, International Symposium Roskilde, N.Hansen *et al.* eds, Risø National Laboratory, Denmark, pp. 74 1-748.